Palaeogeography, Palaeoclimatology, Palaeoecology 509 (2018) 98–104

Contents lists available at ScienceDirect

Palaeogeography, Palaeoclimatology, Palaeoecology

journal homepage: www.elsevier.com/locate/palaeo

Stable carbon isotope records of black carbon on Chinese Loess Plateau since last glacial maximum: An evaluation on their usefulness for paleorainfall and paleovegetation reconstruction

Xu Wang [a,*], Linlin Cui [b], Shiling Yang [a], Jixuan Zhai [a], Zhongli Ding [a]

[a] Key Laboratory of Cenozoic Geology and Environment, Institute of Geology and Geophysics, Chinese Academy of Sciences, P.O. Box 9825, Beijing 100029, China
[b] Institute of Geology and Geophysics, Chinese Academy of Sciences, P.O. Box 9825, Beijing 100029, China

ARTICLE INFO

Article history:
Received 28 October 2016
Received in revised form 24 February 2017
Accepted 2 August 2017
Available online 3 August 2017

Keywords:
Black carbon
Soil organic matter
Carbon isotope composition, C_3/C_4 plants
Rainfall
Chinese Loess Plateau

ABSTRACT

Stable carbon isotope composition of soil organic matter ($\delta^{13}C_{SOM}$) has been widely used to infer past environmental or vegetation (C_3/C_4) changes. However, as a carbonaceous product of incomplete burning of biomass, the carbon isotope signature of black carbon (BC) has received little study and a limited usage on this purpose. Moreover, the environmental or vegetation indication of BC carbon isotope composition ($\delta^{13}C_{BC}$) in sedimentary records remains ambiguous although the $\delta^{13}C_{BC}$ is supposed to reflect carbon isotope composition of vegetation being burnt. This deserves site-specific studies. Here we analyzed $\delta^{13}C_{BC}$ and $\delta^{13}C_{SOM}$ on loess-paleosol samples from Lijiayuan and Yangling sections on Chinese Loess Plateau (CLP) spanning the last glacial maximum to decipher the environmental (or vegetation) meaning of $\delta^{13}C_{BC}$ at each study site. Opposite changing patterns were observed on the $\delta^{13}C_{BC}$ values for the two sections. The $\delta^{13}C_{BC}$ at Yangling (in southern part of the CLP) varied from −19.18‰ to −21.93‰ (mean: −20.62‰) with more positive values occurred during the middle Holocene than those during the LGM, demonstrating more C_4 plants occupied in the region during the warm-humid middle Holocene. This is consistent with the changing pattern widely-documented in $\delta^{13}C_{SOM}$ records over the CLP during the same period. By contrast, the $\delta^{13}C_{BC}$ at Lijiayuan (in northwestern part of the CLP) changed within the range of −21.83‰ ~ −24.64‰ (mean: −23.34‰) and displayed more negative values during the early-middle Holocene with respect to the LGM period. The $\delta^{13}C_{BC}$ at Lijiayuan were about 2.5‰ lower than those at Yangling, indicating a northward decrease of C_4 plants on the CLP. The anti-phased changes of $\delta^{13}C_{BC}$ at Lijiayuan were considered to reflect variations in paleorainfall because the vegetation is dominated by C_3 plants at the study site and carbon isotope compositions of C_3 plants decrease as rainfall increases. Compared with $\delta^{13}C_{SOM}$ record at the same profile, $\delta^{13}C_{BC}$ seem biased against capturing C_4 signal during mid-Holocene possibly due to dominance of C_3 plants at the study site during fire seasons and a potentially extra source of BC from forest fires occurred on surrounding mountains. By contrast, $\delta^{13}C_{BC}$ tend to exaggerate C_4 signal during the LGM attributed to a possible shift of fire season from spring to summer. These findings suggest that we probably underestimate the abundance of C_4 plants during mid-Holocene and overestimate C_4 biomass during the LGM using BC carbon isotope composition.

1. Introduction

Black carbon (BC) is produced from incomplete burning of vegetation and fossil fuels (Goldberg, 1985). BC contains a continuum of materials, ranging from large fragments of slightly charred biomass to microscopic soot and graphitic black carbon (or elemental carbon), which are formed by the condensation of gases produced during combustion (Masiello, 2004). As a product of vegetation fires, BC has been employed to indicate past fire occurrence (Wang et al., 2005, 2012, 2013a). Moreover, BC carbon isotope compositions may demonstrate the type of vegetation that was burned, i.e., C_3/C_4 plants (Bird and Gröcke, 1997) and thus reflect possible environmental changes. Despite its potential proxy value, the $\delta^{13}C$ value of BC ($\delta^{13}C_{BC}$) has received only limited use for past vegetation or environmental reconstruction (e.g., Bird and Cali, 1998; Turney et al., 2001; Jia et al., 2003; Zhou et al., 2009). This is partially because the direct usage of $\delta^{13}C_{BC}$ as paleovegetation reconstruction is still in debate. Major concerns are mainly derived from the observed changes in stable carbon isotopic composition during the combustion process (Wang et al., 2013b) and the influence from exogenous source of BC (Liu et al., 2013). For example, carbon isotope fractionations (CIF) during the conversion of C_3 and C_4 vegetation to BC are highly variable, with a CIF range of −3‰ ~ +3‰ (mean: −0.3‰) for C_3 plants and −10‰ ~ +3‰ (mean: −1.7‰) for C_4

* Corresponding author.
E-mail address: xuking@mail.iggcas.ac.cn (X. Wang).

http://dx.doi.org/10.1016/j.palaeo.2017.08.008
0031-0182/

plants (Wang et al., 2013b). Meanwhile, as for Chinese Loess Plateau, BC produced in desert and surrounding mountains may be carried along with dust and thus affect less BC $\delta^{13}C_{BC}$ values (Liu et al., 2013). Although the above two issues have been addressed and examined in some previous studies (i.e., Wang et al., 2013b; Liu et al., 2013), further assessments are still needed especially from paleorecords covering a broad region with a clear gradient of C_3/C_4 abundances.

Despite BC has encountered the aforementioned major concerns, $\delta^{13}C_{BC}$ still has some advantages over $\delta^{13}C_{SOM}$ in application to past vegetation or environmental reconstruction. These advantages are as followed: (1) the $\delta^{13}C_{SOM}$ can be potentially biased by pre-analysis acid preparation (Brodie et al., 2011). By contrast, BC is chemically inert and resistant to alteration by acid treatment (Bird and Cali, 1998); (2) pedogenic degradation may exert additional effect on $\delta^{13}C_{SOM}$ (Zech et al., 2007) whereas BC is also biochemically inert enough to resist to biodegradation (Masiello, 2004); (3) the interpretation of $\delta^{13}C_{SOM}$ from loess-paleosol sequences can be challenging because multiple factors can influence $\delta^{13}C_{SOM}$ (Zech et al., 2013). In this context, it deserves more $\delta^{13}C_{BC}$ analysis in sedimentary records to facilitate our meaningful interpretation for it.

The loess deposits on Chinese Loess Plateau (CLP) have been recognized as an ideal archive for paleofire studies using BC abundance (Wang et al., 2005). This is because the completeness and continuity of loess deposition enable stratigraphical correlation between far-located loess sections (Ding et al., 2002). We therefore choose Chinese loess-paleosol sequences to examine the effectiveness of $\delta^{13}C_{BC}$ record as an indicator of paleo-environment and paleo-vegetation reconstruction. Moreover, $\delta^{13}C_{SOM}$ records have been intensively applied to infer the changes in abundances of C_3/C_4 plants over the CLP especially since the last glacial maximum (LGM) (Yang et al., 2015). The research results would help us better understand usage of $\delta^{13}C_{BC}$ record.

In this study, we measured $\delta^{13}C_{BC}$ on loess-paleosol profiles spanning the LGM and the Holocene from Lijiayuan and Yangling sections, which are located in northwestern and southern part of the CLP, respectively. We compared the $\delta^{13}C_{BC}$ records with $\delta^{13}C_{SOM}$ records from the same profiles, with the objective to examine the differences between the two proxies in constraining past environmental or vegetation changes.

2. Study area

The Lijiayuan section (36°7′0″N, 104°51′30″E) is located to the north of Huining County, Gansu Province in the northwestern part of the Loess Plateau and is ~100 km from the modern desert margin (Fig. 1). At present, the mean annual temperature is ~7 °C at the site, with a July average of 22.6 °C and a January average of −7.7 °C. The mean annual precipitation is ~250 mm, and about 70% of the rainfall occurs in summer. The Yangling section (34°17′24″N, 108°5′24″E) is situated in southern part of the Loess Plateau (Fig. 1). The mean annual temperature is ~13 °C, with a July average of 26.1 °C and a January average of −1.2 °C. The mean annual precipitation is ~650 mm at the site, and about 50% of the rainfall occurs in summer. These two study sites stride from semi-humid to semi-arid area and possess far different climatic conditions, allowing for site-specific studies.

For both the study areas, most of rainfall occurs in summer, brought by the East Asia summer monsoon. In winter, the prevailing winds are northwesterly and generate frequent dust storms due to the high pressure over Siberia.

The stratigraphic divisions for these two sections have been made based on grain size, magnetic susceptibility and the pedogenic characteristics (Fig. 2), following the method of Yang and Ding (2008). Both sections consist of soil unit S_0 and the upper part of loess unit L_1. The Holocene soil (S0), overlain by modern topsoil, is dark in color because of its relatively high organic matter content. Loess unit L1, yellowish in color and massive in structure, was deposited during the last glacial period. L1 can be generally divided into five subunits termed L1-1, L1-2, L1-3, L1-4 and L1-5. Among them, L1-2 and L1-4 are weakly developed soil whereas the others are typical loess. Previous studies (Kukla, 1987; Lu et al., 1987; Ding et al., 2002; Lu et al., 2007) have shown that L1-1 is correlated with MIS 2 (~27–11 ka) and S0 corresponds to the early-mid Holocene (~11–3 ka).

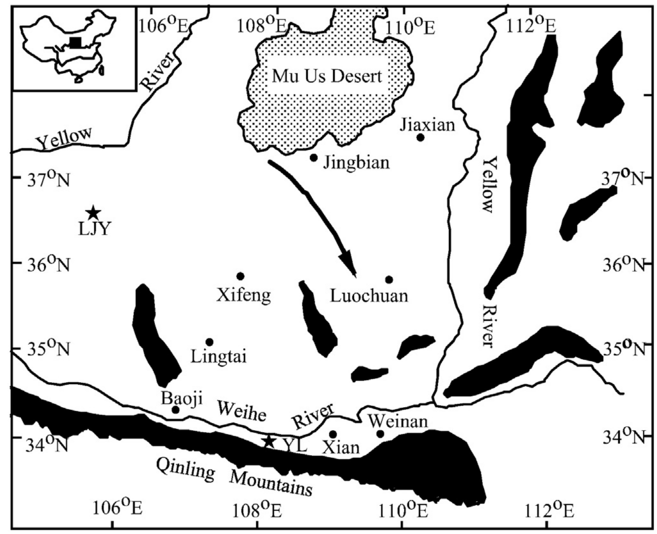

Fig. 1. Location map showing the localities of the studied sections labeled as stars (LJY-Lijiayuan; YL-Yangling). The arrow indicates the dominant subaerial wind direction in winter season, coinciding with the observed decrease in grain size and thickness of loess. The desert (dotted area) and mountains (black areas) around and within the Loess Plateau are shown. The solid square in the inset map shows the locality of the Loess Plateau in continental China.

3. Materials and methods

For Lijiayuan section, we took loess and paleosol samples at ~10 cm interval and a total of 84 samples were collected above 7.26 m in depth, spanning the Holocene and late last glacial period. Only $\delta^{13}C$ of BC was measured here and a total of 84 $\delta^{13}C_{BC}$ data were obtained for Lijiayuan section. The $\delta^{13}C_{SOM}$ data for Lijiayuan section (namely Huining section) were cited from Yang et al. (2015) for a purpose of comparison. For Yangling section, we took loess and paleosol samples at 5 cm interval and a total of 85 samples were collected for the period over late last glacial time. We measured $\delta^{13}C$ on both BC and soil organic matter (SOM) for the same profile on the purpose of comparison. A total of 64 samples for BC and 64 samples for SOM were determined for carbon isotope.

We used the chemical oxidation method developed by Lim and Cachier (1996) to extract the BC in the loess–soil samples. In brief, the carbonates and part of the silicates in the samples were removed by an acid treatment with HCl (3 mol/L) and HF (10 mol/L)/HCl (1 mol/L) in sequence. The treated samples were then oxidized by a solution of 0.1 mol/L $K_2Cr_2O_7$/2 mol/L H_2SO_4 at 55 °C for 60 h to remove soluble organic matter and kerogen. After the treatment, the remaining refractory carbon in the residue is called BC, and includes charcoal and the atmospheric BC particles from regional fires as well as other sources besides fire (Lim and Cachier, 1996).

For SOM extraction, samples (~2.5 g) were first screened for modern rootlets and then digested for 48 h in diluted (1 mol/L) HCl at room temperature to remove carbonate. The diluted HCl was used just in case some labile organic compounds would be lost during chemical pretreatment using more concentrated acid. The residue were then washed to pH >5 with distilled water and dried cryogenically at −80 °C using freeze drying machine.

The $\delta^{13}C$ analyses were performed on a continuous-flow isotope ratio mass spectrometer (CF-IRMS). The CF-IRMS system consists of an elemental analyzer (Flash 1112 series) coupled to a Finnigan MAT 253 mass spectrometer. The standard samples with known $\delta^{13}C$ value

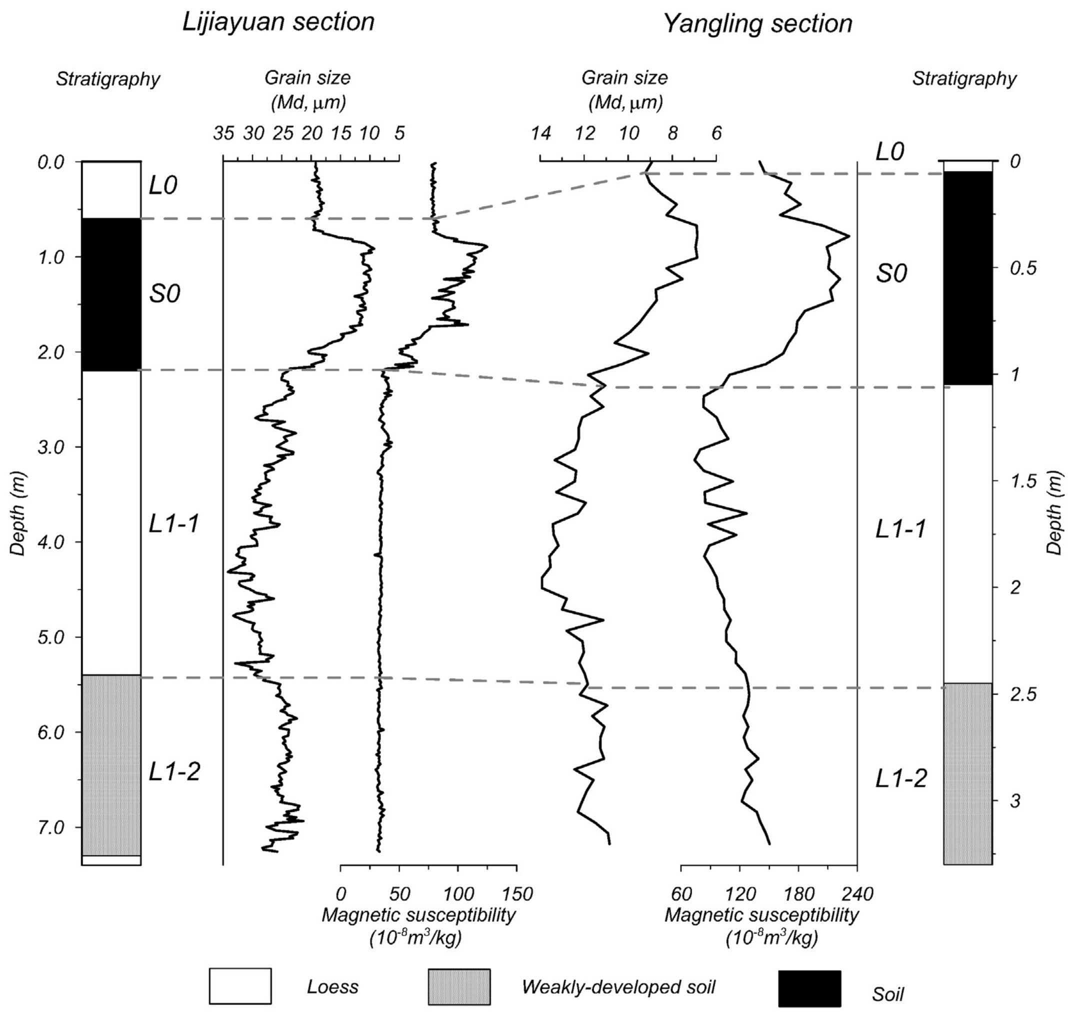

Fig. 2. Sub-division of stratigraphic units in each section based on median grain size and magnetic susceptibility curves. The grain size and magnetic susceptibility data for Yangling and Lijiayuan were cited from Zhao and Ding (2014) and Yang et al. (2015), respectively.

(e.g., Glycine: $\delta^{13}C_{VPDB} = -33.3‰$) were used to monitor the measurement. Analytical precisions were better than $\pm 0.2‰$.

4. Results

The variations in $\delta^{13}C_{BC}$ compared with the $\delta^{13}C_{SOM}$ records for both Lijiayuan and Yangling sections are displayed in Fig. 3. The $\delta^{13}C_{BC}$ values for Lijiayuan section range from −21.83 to −24.64‰, with an average of −23.36‰. The $\delta^{13}C_{BC}$ at Lijiayuan showed more positive values (mean: −22.80‰) during the LGM period and then decreased during Holocene with the most negative of −24.64‰ at mid-Holocene. By contrast, the $\delta^{13}C_{BC}$ for Yangling section varied from −19.18‰ to −21.93‰ (mean: −20.62‰), being obviously higher than those for Lijiayuan. Meanwhile, the $\delta^{13}C_{BC}$ at Yangling were relatively more negative during the LGM period than during the Holocene, i.e., a mean $\delta^{13}C_{BC}$ of −21.01‰ during the LGM and −19.61‰ at mid-Holocene, showing a reverse phase of change compared to that of Lijiayuan.

Comparatively, the $\delta^{13}C_{SOM}$ records for the two sections shared a common feature and demonstrated a consistent increase from the LGM to the Holocene. For example, the $\delta^{13}C_{SOM}$ fall in the range of −23.75‰ to −20.74‰ for the LGM loess unit and within the range of −22.58‰ to −18.94‰ for the Holocene soil. Moreover, they exhibited a good correlation with the grain size and magnetic susceptibility records. For example, more positive $\delta^{13}C_{SOM}$ values correspond to finer grain size and higher magnetic susceptibility, and vice versa.

5. Discussion

5.1. Carbon isotope compositions of BC on CLP and C_3/C_4 vegetation reconstruction

It is well known that plants use two principal photosynthetic pathways to fix carbon, C_3 and C_4, which have apparently different carbon isotope signatures (Deines, 1980; O'Leary, 1988; Farquhar et al., 1989). For instance, an investigation of modern plants in the loess region of North China (Wang et al., 2008a) has shown that C_3 plants have $\delta^{13}C$ values ranging from −21.7‰ to −30‰ with a mean of −26.7‰ whereas C_4 plants have $\delta^{13}C$ values of −10‰ ~ −15.8‰ (mean: −12.8‰). To date, $\delta^{13}C_{SOM}$ records generated from loess-paleosol sections have been widely used to infer past C_3/C_4 vegetation changes (e.g., Gu et al., 2003; Liu et al., 2005; Rao et al., 2005; Wang et al., 2008a; Yang et al., 2015). The general features are that relative abundance of C_4 plants increased on CLP from the last glacial to mid-Holocene and decreased northwestward on CLP during both the last glacial and mid-Holocene.

In order to estimate C_3/C_4 biomass over the LGM period using our $\delta^{13}C_{BC}$ or $\delta^{13}C_{SOM}$ records, we basically followed the method developed by Yang et al. (2015), which considered the effects of the carbon isotope composition of atmospheric CO_2, precipitation and temperature change on the $\delta^{13}C$ values of C_3 and C_4 plants. After correcting for these factors, the end-member $\delta^{13}C$ values for C_3 ($\delta^{13}C_{C3}$) and C_4 plants ($\delta^{13}C_{C4}$) were obtained as followed: $\delta^{13}C_{C3} = -24.0‰$ and $\delta^{13}C_{C4} = -10.1‰$ for Holocene whereas $\delta^{13}C_{C3} = -24.1‰$ and $\delta^{13}C_{C4} = -10.2‰$ for the LGM.

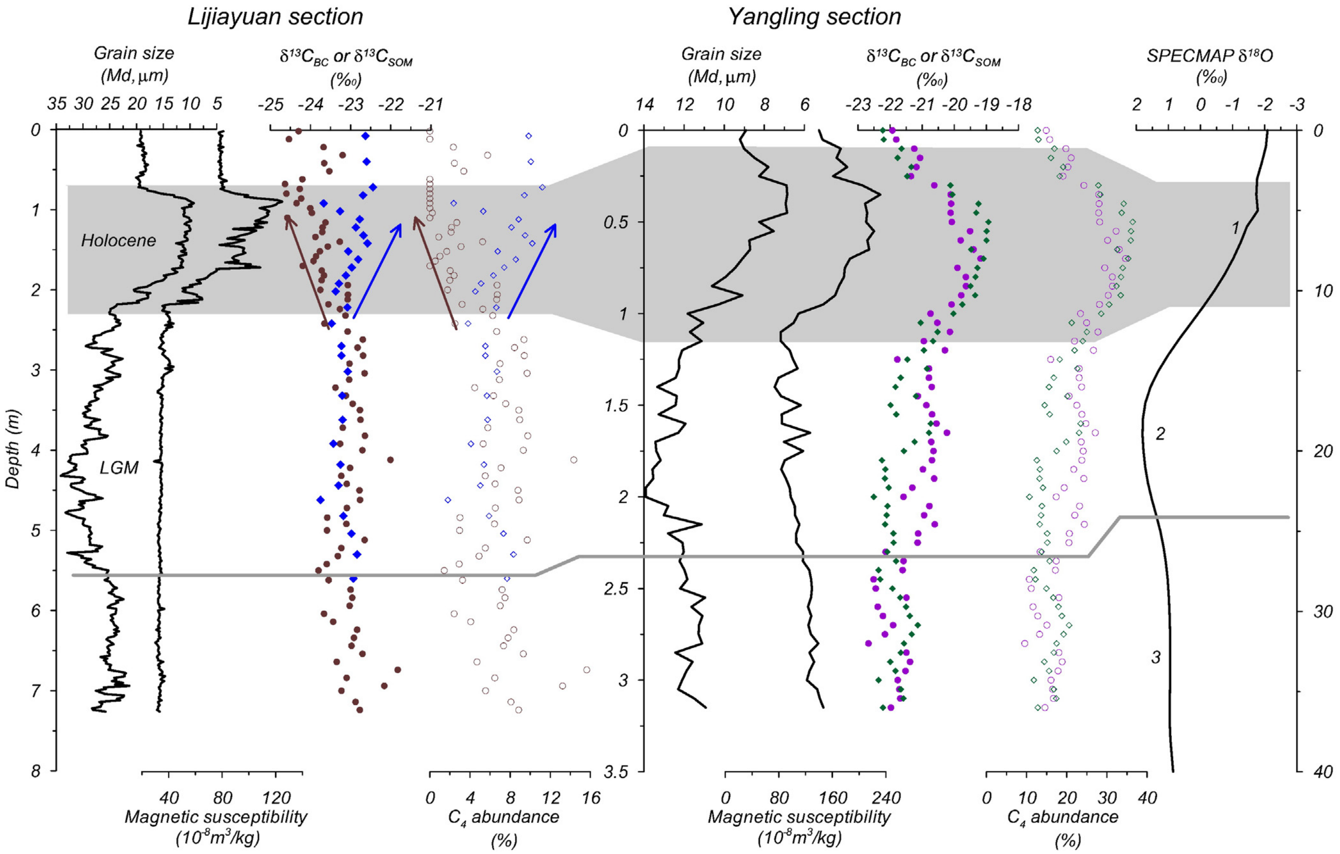

Fig. 3. A comparison of $\delta^{13}C_{BC}$ with $\delta^{13}C_{SOM}$ records and changes in inferred C_4 abundances since the LGM for Lijiayuan ($\delta^{13}C_{BC}$: brown solid circles, $\delta^{13}C_{SOM}$: blue solid circles, $\delta^{13}C_{BC}$-derived C_4 abundance: brown open circles, $\delta^{13}C_{SOM}$-derived C_4 abundance: blue open circles) and Yangling ($\delta^{13}C_{BC}$: purple solid circles, $\delta^{13}C_{SOM}$: green solid diamonds, $\delta^{13}C_{BC}$-derived C_4 abundance: purple open circles, $\delta^{13}C_{SOM}$-derived C_4 abundance: green open diamonds). Note that the $\delta^{13}C_{BC}$ showed an opposite trend during the transition from the LGM to the Holocene with respect to the $\delta^{13}C_{SOM}$ record at Lijiayuan (as arrows indicated). Accordingly, the $\delta^{13}C_{BC}$ record at Lijiayuan yielded an apparently underestimated C_4 biomass during mid-Holocene as compared with the $\delta^{13}C_{SOM}$ record. The $\delta^{13}C_{SOM}$ data for Lijiayuan section was cited from Yang et al. (2015). The SPECMAP time scale was cited from Imbrie et al. (1984).

C_4 plant abundance was calculated by applying the measured $\delta^{13}C$ values to an isotope mass-balance equation: $C_4\ (\%) = [(\delta^{13}C - \delta^{13}C_{C3})/(\delta^{13}C_{C3} - \delta^{13}C_{C4})] \times 100$.

The changes in C_4 biomass over the LGM estimated using $\delta^{13}C_{BC}$ and $\delta^{13}C_{SOM}$ records were shown in Fig. 3. At Lijiayuan in northwestern part of CLP, $\delta^{13}C_{BC}$-derived C_4 plant abundance decreased from a mean of 5.8% to 1.1% from the LGM to mid-Holocene. Conversely, $\delta^{13}C_{SOM}$-derived C_4 plant abundance increased from a mean of 5.8% to 8.1% during the same time intervals. By contrast, at Yangling in southeastern part of CLP, $\delta^{13}C_{BC}$-derived C_4 plant abundance increased from a mean of 22.9% to 30.4% from the LGM to mid-Holocene. At the same time, $\delta^{13}C_{SOM}$-derived C_4 plant abundance at Yangling showed the same changing pattern, i.e., an increase from a mean of 17.8% to 33.6% during the same time intervals. Spatially, both $\delta^{13}C_{SOM}$ and $\delta^{13}C_{BC}$-derived C_4 plant abundances displayed a northwestward decrease over the CLP, which is consistent with the northwest-southeast zonal distribution pattern of C_4 biomass observed in $\delta^{13}C_{SOM}$ records (Yang et al., 2015). However, with regard to the temporal changing pattern, the $\delta^{13}C_{BC}$-derived C_4 plant abundance at Lijiayuan exhibited a reversed phase of change in comparison to the general feature of glacial-interglacial C_4 biomass shift gained in $\delta^{13}C_{SOM}$ records from loess sections. This difference may indicate that carbon isotope composition of BC at Lijiayuan possibly documented a variation in environmental signal rather than a C_3/C_4 vegetation change. This deserves a detailed discussion as below.

The $\delta^{13}C_{SOM}$ record showed that C_4 biomass was <10% at Lijiayuan since the LGM. That is to say C_3 plants dominated in the region during both the LGM and mid-Holocene. It could be explained by low growing season temperature at the study site. Previous studies have shown that higher growing season temperature and enhanced summer precipitation favor C_4 over C_3 plants (Sage et al., 1999; Gu et al., 2003; Liu et al., 2005; Yang et al., 2012). However, C_4 plant abundance in North China is mainly controlled by temperature, i.e., the percentage of C_4 plants was significantly lower below the 22° isotherm of the warmest month (Auerswald et al., 2009; Wittmer et al., 2010). The average temperature of ~22.6 °C for July, the warmest month at Lijiayuan, is quite close to the above threshold temperature, which may account for the low abundance of C_4 plants in the modern vegetation of the region.

Some surveys on modern ecosystems in North China have found that carbon isotope compositions of C_3 plants shifted towards more negative values along with the increase of mean annual precipitation (Wang et al., 2003; Liu et al., 2005). The considerable increase in mean annual precipitation during mid-Holocene should cause negative shift of C_3 plant $\delta^{13}C$ values, which would be certainly reflected in both $\delta^{13}C_{BC}$ and $\delta^{13}C_{SOM}$ records if regional vegetation was composed of pure C_3 plants. However, in the region still occupied by a small portion of C_4 plants as shown in $\delta^{13}C_{SOM}$ record, this negative shift signal was surprisingly documented in $\delta^{13}C_{BC}$ record. This means that BC carbon isotope compositions tend to bias the real C_3/C_4 signature, especially in the region predominated by C_3 plants. It can be explained by the seasonality of fire occurrence. In North China, nature fires mainly occur in dry seasons, i.e., spring and winter (Li, 2006; Zhang et al., 2007; Wang et al., 2012). For a specific site, the peak of C_3 and C_4 plant metabolism differs seasonally (Ode et al., 1980). High C_4 component occurs in summer at the CLP due to relatively high temperature and enhanced precipitation (Yang et al., 2012). Since black carbon (as a product of fires) is mainly produced in spring and winter, covering a period of C_3 plant growth, its $\delta^{13}C$ value is biased towards a C_3 signal. Therefore, the C_4

biomass estimated from $\delta^{13}C_{BC}$ values should be regarded as lower limits. This is especially the case during mid-Holocene based on a comparison between the C_4 abundances derived from $\delta^{13}C_{BC}$ and $\delta^{13}C_{SOM}$ records, i.e., 1.1% versus 8.1% for Lijiayuan and 30.4% versus 33.6% for Yangling during the period (Fig. 3).

At the same time, in contrast to the soil organic matter that records the local floral biomass, the BC tends to document floral components from a vast area because it could transport for a long distance as entrained by fire convection flows (Wang et al., 2013a). Modern landscape in our study area is semiarid steppe (Chen, 1987). The vegetation is characterized by herbs, shrubs, and deciduous broad-leaved trees. The dominant herbs include *Artemisia*, *Stipa*, *Achnatherum*, *Cleistogenes*, *Typha*, and *Ephedra*, together with such xerophytic herbs as *Peganum* and *Agriophyllum* (Department of Geography, Shaanxi Normal University, 1987). The dominant elements of deciduous broad-leaved trees include *Betula*, *Quercus*, *Salix*, *Ulmus*, and *Alnus*, which only grow on undisturbed loess hills because of a long history of crop planting. During the mid-Holocene, temperate coniferous and broad-leaved forest developed in the western part of CLP (Li et al., 2006; Tang et al., 2007; Sun et al., 2010). In this case, forest fires occurred on surrounding mountains may provide an extra source of BC, which would further exaggerate C_3 signal in the carbon isotope record in northwestern CLP. This is also the case for southeastern part of CLP, where more tree vegetation developed during the mid-Holocene than in the northwestern part due to relatively high rainfall amount (Jiang et al., 2013; Jiang et al., 2014). However, this may cause limited influence on the $\delta^{13}C_{BC}$-derived C_4 abundance because C_4 plants were also abundant along with the enhanced summer rainfall under favorable temperature condition in southeastern CLP. This can be envisaged in the relatively small contrast between $\delta^{13}C_{BC}$-derived and $\delta^{13}C_{SOM}$-derived C_4 abundances at Yangling (Fig. 3).

Another difference between $\delta^{13}C_{BC}$ and $\delta^{13}C_{SOM}$ records lies in that they may document different temporal periods of vegetation or environmental changes. Since soil organic matters accumulate continuously along with time in loess-paleosol deposit, $\delta^{13}C_{SOM}$ of each sample represents an integration of vegetation or environmental changes at a certain time period covered by each sampling interval. By contrast, BC incorporate into loess-paleosol deposit during the years of fire occurrence under dry conditions and therefore $\delta^{13}C_{BC}$ of each sample only records vegetation or environmental changes in the fire years within a certain time period covered by each sampling interval. For the studied profiles of Lijiayuan and Yangling, each sample represents a time interval of 300–600 years, which may witness multiple fire episodes. This thus ensures a general resemblance between $\delta^{13}C_{BC}$ and $\delta^{13}C_{SOM}$ records if the carbon for BC and SOM are from the same sources. It can be seen in the $\delta^{13}C_{BC}$ and $\delta^{13}C_{SOM}$ records of Yangling profile (Fig. 3). However, some differences can also be observed on the two records, i.e., negative shifts of $\delta^{13}C_{BC}$ with respect to $\delta^{13}C_{SOM}$ under warm/humid conditions during mid-Holocene and MIS 3 stage as well as positive shifts of $\delta^{13}C_{BC}$ with respect to $\delta^{13}C_{SOM}$ under cold/dry conditions during LGM. These different offsets may be explained by changed seasonality of fire occurrences during the different climatic periods. During glacial periods like LGM, the East Asian summer monsoon is weaker, with precipitation narrowly focused within the summer or part of the summer (Yang et al., 2012). This could reduce plant productivity and thus lead to low fuel loads in spring and autumn due to low precipitation amount, which would suppress fire occurrences during these seasons. By contrast, relatively high fuel loads and dry conditions during non-rainy days in the summer could promote fire occurrence, which would produce more BC from C_4 biomass and therefore make $\delta^{13}C_{BC}$ shift towards more positive values with respect to $\delta^{13}C_{SOM}$. During interglacial periods like mid-Holocene and MIS 3 stage, intensified summer monsoon resulted in high precipitation and a long rainy season (Yang et al., 2012), which may exclude fires from happening in summer. In this case, the fires occurred in spring and autumn may generate more BC from C_3 biomass, which therefore makes $\delta^{13}C_{BC}$ shift to more negative values as compared with $\delta^{13}C_{SOM}$.

In addition, potential overprint of paleo-environmental records by root is also an important influencing factor, which might be applicable to $\delta^{13}C_{SOM}$ record due to undiscernible carbonized root debris despite we carefully picked out modern rootlet. Nevertheless, this overprint could be ruled out by $\delta^{13}C_{BC}$ record because the above-mentioned root carbon was digested by chemical oxidation during extraction process of BC. This may partially contribute to the observed differences between $\delta^{13}C_{BC}$ and $\delta^{13}C_{SOM}$ records.

Collectively, we may to some extent either underestimate the abundance of C_4 plants during interglacial periods or overestimate the abundance of C_4 plants during glacial periods when BC carbon isotope record was used to infer C_3/C_4 abundances.

5.2. Inferring precipitation based on the $\delta^{13}C_{BC}$ record at Lijiayuan

Because the carbon isotope compositions of BC mainly reflect a negative isotopic response of C_3 plants to precipitation at Lijiayuan, we attempt to reconstruct precipitation using the $\delta^{13}C_{BC}$ values in this study. In the process of precipitation reconstruction, the influence of changes in trees versus C_3 grasses on $\delta^{13}C_{BC}$ values would be neglected since the $\delta^{13}C$ difference between trees and C_3 grasses has not been well constrained so far. Moreover, on the CLP, a maximum difference of ~1‰ was observed on them (Zheng and Shangguan, 2007), which would result in a limited variation in BC carbon isotope compositions. To reconstruct precipitation, we employed the leaf ^{13}C discrimination (Δ_{leaf}), which takes the changing $\delta^{13}C$ value of atmospheric CO_2 ($\delta^{13}C_{air}$) into consideration. The Δ_{leaf} values were calculated using the following equation: $\Delta_{leaf} = (\delta^{13}C_{air} - \delta^{13}C_{leaf})/(1 + \delta^{13}C_{leaf}/10^3)$. The $\delta^{13}C_{leaf}$ represents the $\delta^{13}C$ value of leaf or plant, which was directly estimated from $\delta^{13}C_{BC}$. The $\delta^{13}C_{air}$ value after 17.4 ka BP was inferred by interpolating values from Antarctic ice-core records and modern observation data from Antarctic stations as described in Ferrio et al. (2005). The inferred $\delta^{13}C_{air}$ values vary between −6.3‰ and −7.7‰. For the $\delta^{13}C_{air}$ values during 17.4–27.5 ka BP, we adopted a value of −6.6‰ because carbon isotope compositions of CO_2 trapped in Antarctic ice cores at this time period varied in a very narrow range, i.e., from −6.4‰ to −6.8‰ (Lourantou et al., 2010).

Some recent studies (Diefendorf et al., 2010; John, 2010) have observed a strong positive correlation between Δ_{leaf} and mean annual precipitation (MAP) at the global scale. To reconstruct past precipitation, we should choose a proper transfer function to translate the Δ_{leaf} values to precipitation changes at our study site. We then used an established transfer function by Wang et al. (2013b) that is based on the published carbon isotopic data for C_3 plants in North China (Wang et al., 2008a). The reconstructed changes in annual precipitation at Lijiayuan over the late last glacial are shown in Fig. 4. Our results indicate that the inferred annual precipitation varied from ca. 100 mm to 367 mm over the past 27.5 ka. During the pre-LGM and LGM periods (27.5 to 14.6 ka BP), reconstructed annual precipitations were relatively low with most values <230 mm (averaged at 208 mm), indicative of a dry climate prevailed over the region. From last deglacial to mid-Holocene (14.6 to 4.0 ka BP), the annual precipitation showed a gradual increase, with the highest value of 367 mm occurred at 4.0 ka BP. During the late Holocene (4.0 ka BP to present), precipitation sharply declined to about 242 mm by 1.6 ka BP and then increased to 359 mm at 0.6 ka BP. The topmost sample at the Lijiayuan profile yielded a precipitation of 219 mm, consistent with the present-day value of 250 mm, which supports our methodology.

According to our results, the inferred precipitation exhibited a gradual increase during the transition from the LGM to the Holocene, which was attributed to progressive enhancement of East Asia summer monsoon as envisaged in the gradually negative shift of stalagmite $\delta^{18}O$ data in south China (Fig. 4). The same trend of changes in the reconstructed precipitation was also observed in other study sites in western CLP (Rao et al., 2013). Meanwhile, mid-Holocene was characterized by maximum precipitation throughout the record, which means a humid

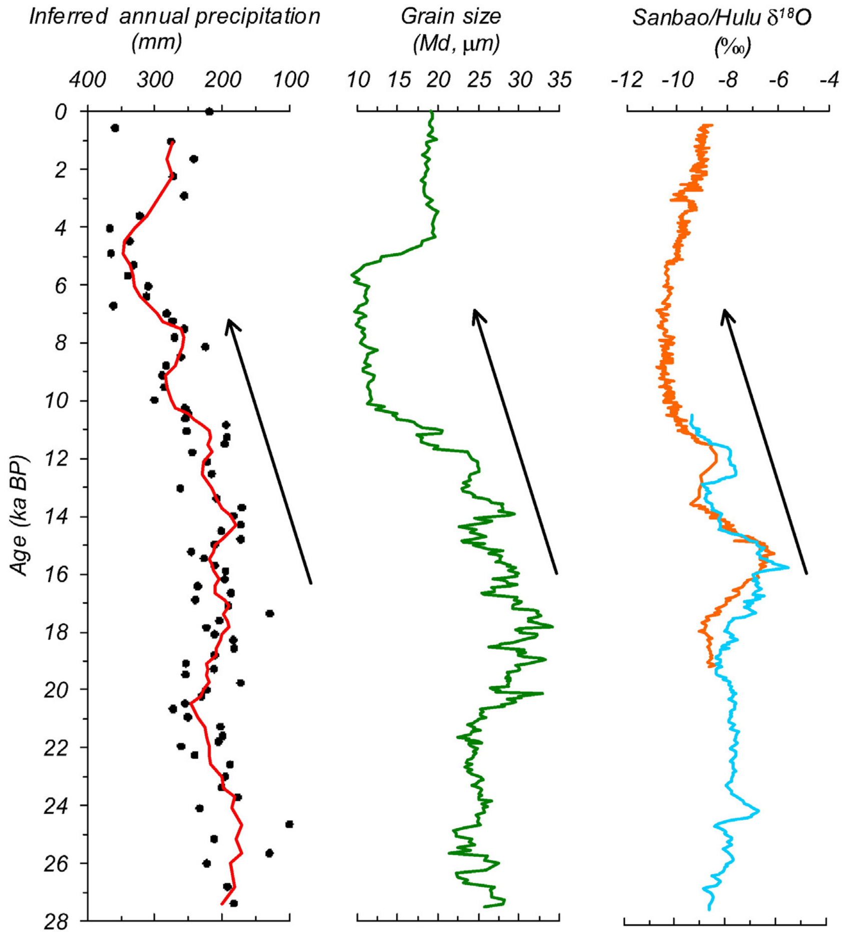

Fig. 4. The variation of annual precipitation since 27.5 ka BP inferred using $\delta^{13}C_{BC}$ record at Lijiayuan site, in comparison with grain size in the same section and Sanbo/Hulu stalagmite $\delta^{18}O$ data values in central China. The Hulu $\delta^{18}O$ record (orange) is plotted 1.6‰ more negative to account for the higher Hulu values than Sanbao cave (blue) (see Wang et al., 2008b). The time scale for Lijiayuan section is cited from Wang et al. (2012), which was obtained using orbital tuning method.

climate at northwestern part of CLP. This observation is in accordance to the formerly inferred warm and humid climate during middle Holocene in the region (An et al., 2003, 2006; Feng et al., 2004; Sun et al., 2010). This favorable climate promotes the Yangshao Culture (6800–4900 cal. years BP) developed on the western Loess Plateau (Shui, 2001) and the intensified land use as indicated by frequent human fires at Lijiayuan site (Wang et al., 2012). Moreover, the timing of highest precipitation in our record may suggest East Asia summer monsoon have not reached its peak intensity at our study site until 4.0 ka BP. By contrast, the peak summer monsoon was witnessed much earlier in some areas to the east of Lijiayuan site, i.e., maximum precipitation occurred at a period of 7000–6500 yr BP in Daihai lake region (Xiao et al., 2006). This may suggest a progressive strengthening of the summer monsoon during the middle Holocene towards inland direction. However, we cannot rule out potential effects of biotubation during the humid condition of mid-Holocene, which may cause a diffusion of the $\delta^{13}C_{BC}$ and $\delta^{13}C_{SOM}$ records and therefore influence the timing of the inferred peak precipitation. After 4.0 ka BP, the precipitation rapidly decreased at our study site, which shows consistence with the onset of drying over the Loess Plateau (An et al., 2003, 2006; Feng et al., 2004). All in all, BC carbon isotope composition at Lijiayuan can serve as a reliable proxy to monitor changes in monsoonal precipitation.

6. Conclusion

In this study, we made a systematic comparison between the carbon isotopic records of black carbon and soil organic matter ($\delta^{13}C_{BC}$ vs. $\delta^{13}C_{SOM}$) since last glacial maximum at the Yangling and Lijiayuan sites along a southeast to northwest transect on Chinese Loess Plateau. Our results demonstrated that the $\delta^{13}C_{BC}$ record could document the same changing pattern of C_4 abundances as the $\delta^{13}C_{SOM}$ record did at Yangling in southeast part of CLP, occupied by mixed C_3/C_4 vegetation. By contrast, the $\delta^{13}C_{BC}$ record registered a precipitation signature rather than the C_3/C_4 variation as shown in the $\delta^{13}C_{SOM}$ record at Lijiayuan especially during mid-Holocene in northwest part of CLP, where C_3 plants dominated. By comparing $\delta^{13}C_{BC}$ with $\delta^{13}C_{SOM}$ from the same profile of Yangling, we found that $\delta^{13}C_{BC}$ were generally more negative than $\delta^{13}C_{SOM}$ during mid-Holocene and MIS 3 stage and less negative than $\delta^{13}C_{SOM}$ during LGM. The different offset between $\delta^{13}C_{BC}$ and $\delta^{13}C_{SOM}$ from LGM to the Holocene may be mainly attributed to different seasonality of fire occurrence during different climatic periods, which causes more C_3 vegetation being burnt in fire seasons during the mid-Holocene and more C_4 vegetation being burnt in fire season during the LGM. Moreover, black carbon produced from forest fires occurred on surrounding mountains may also contribute to enhance C_3 signal in the $\delta^{13}C_{BC}$ record during the mid-Holocene. In this case, BC carbon isotope composition tends to underestimate the relative abundance of C_4 plants during the mid-Holocene and overestimate the relative abundance of C_4 plants during the LGM. This suggests a restricted usage of for paleovegetation reconstruction. However, the $\delta^{13}C_{BC}$ record generated from the loess region dominated by C_3 plants may be a useful proxy indicator for precipitation changes. This receives testified by our $\delta^{13}C_{BC}$ record at Lijiayuan site.

Acknowledgements

This research was financially supported by the Strategic Priority Program of the Chinese Academy of Sciences (grant number XDPB05) and National Natural Science Foundation of China (grant number 41572163 and 41603013). We are grateful to two anonymous reviewers for constructive comments on an early version of the manuscript.

References

An, C.B., Feng, Z.D., Tang, L.Y., 2003. Evidence of humid mid-Holocene in the western part of the Chinese Loess Plateau. Chin. Sci. Bull. 48, 2472–2479.

An, C.B., Feng, Z.D., Barton, L., 2006. Dry or humid? Mid-Holocene humidity changes in arid and semi-arid China. Quat. Sci. Rev. 25, 351–361.

Auerswald, K., Wittmer, M.H.O.M., Männel, T.T., Bai, Y.F., Schäufele, R., Schnyder, H., 2009. Large regional-scale variation in C3/C4 distribution pattern of Inner Mongolia steppe is revealed by grazer wool carbon isotope composition. Biogeosciences 6, 795–805.

Bird, M.I., Cali, J.A., 1998. A million-year record of fire in sub-Saharan Africa. Nature 394, 767–769.

Bird, M.I., Gröcke, D.R., 1997. Determination of the abundance and carbon isotope composition of elemental carbon in sediments. Geochim. Cosmochim. Acta 16, 3413–3423.

Brodie, C.R., Leng, M.J., Casford, J.S.L., Kendrick, C.P., Lloyd, J.M., Zong, Y.Q., Bird, M.I., 2011. Evidence for bias in C and N concentrations and $\delta^{13}C$ composition of terrestrial and aquatic organic materials due to pre-analysis acid preparation methods. Chem. Geol. 282, 67–83.

Chen, C.Y., 1987. A preliminary study of climate and vegetation types in loess plateau, Gansu province. J. Nat. Resour. 2, 347–358 (in Chinese with English abstract).

Deines, P., 1980. The isotopic composition of reduced organic carbon. In: Fritz, P., Fontes, J.C. (Eds.), Handbook of Environmental Isotope Geochemistry. Elsevier, Amsterdam, pp. 329–406.

Department of geography, Shaanxi Normal University, 1987. Geography of Yulin, Shaanxi Province. Shaanxi People's Press, Xian 351 pp.

Diefendorf, A.F., Mueller, K.E., Wing, S.L., Koch, P.L., Freeman, K.H., 2010. Global patterns in leaf 13C discrimination and implications for studies of past and future climate. Proc. Natl. Acad. Sci. U. S. A. 107, 5738–5743.

Ding, Z.L., Derbyshire, E., Yang, S.L., Yu, Z.W., Xiong, S.F., Liu, T.S., 2002. Stacked 2.6-Ma grain size record from the Chinese loess based on five sections and correlation with the deep-sea ^{18}O record. Paleoceanography 17 (3):1033. http://dx.doi.org/10.1029/2001PA000725.

Farquhar, G.D., Ehleringer, J.R., Hubick, K.T., 1989. Carbon isotope discrimination and photosynthesis. Annu. Rev. Plant Physiol. Plant Mol. Biol. 40, 503–537.

Feng, Z.D., An, C.B., Jull, A.T., Tang, L.Y., 2004. Stratigraphic evidence of the mid-Holocene Magehumid climate in the western part of Chinese Loess Plateau. Glob. Planet. Chang. 43, 145–155.

Ferrio, J.P., Araus, J.L., Buxó, R., Voltas, J., Bort, J., 2005. Water management practices and climate in ancient agriculture: inference from the stable isotope composition of archaeobotanical remains. Veg. Hist. Archaeobotany 14, 510–517.

Goldberg, E.D., 1985. Black Carbon in the Environment. John Wiley & Sons, New York.

Gu, Z.Y., Liu, Q., Xu, B., Han, J.M., Yang, S.L., Ding, Z.L., Liu, T.S., 2003. Climate as the dominant control on C_3 and C_4 plant abundance in the Loess Plateau: organic carbon isotope evidence from the last glacial-interglacial loess-soil sequences. Chin. Sci. Bull. 48, 1271–1276.

Imbrie, J., Hays, J.D., Martinson, D.B., McIntyre, A., Mix, A.C., Morley, J.J., Pisias, N.G., Prell, W.L., Shackleton, N.J., 1984. The orbital theory of Pleistocene climate: support from a revised chronology of the marine delta ^{18}O record. In: Berger, A., Imbrie, J., Hays, J., Kukla, G., Saltzman, B. (Eds.), Milankovitch and Climate. Part I. Reidel Publishing Co., Boston, pp. 269–305.

Jia, G.D., Peng, P.A., Zhao, Q.H., Fu, J.M., 2003. Changes in terrestrial ecosystem since 30 Ma in East Asia: stable isotope evidence from black carbon in the South China Sea. Geology 31, 1093–1096.

Jiang, W.Y., Cheng, Y.F., Yang, X.X., Yang, S.L., 2013. Chinese Loess Plateau vegetation since the Last Glacial Maximum and its implications for vegetation restoration. J. Appl. Ecol. 50 (2), 440–448.

Jiang, W.Y., Yang, X.X., Cheng, Y.F., 2014. Spatial patterns of vegetation and climate on the Chinese Loess Plateau since the Last Glacial Maximum. Quat. Int. 334 (335), 52–60.

John, M.J., 2010. Carbon isotope compositions of terrestrial C3 plants as indicators of (paleo)ecology and (paleo)climate. Proc. Natl. Acad. Sci. U. S. A. 107, 19691–19695.

Kukla, G., 1987. Loess stratigraphy in central China. Quat. Sci. Rev. 6, 191–219.

Li, G.L., 2006. Monitor and control techniques of grassland fire in Gansu province. Pratacultural Sci. 23, 87–91 (in Chinese with English abstract).

Li, C.H., Tang, L.Y., Feng, Z.D., Zhang, H.C., Wang, W.G., An, C.B., 2006. A high-resolution late Pleistocene record of pollen vegetation and climate change from Jingning, NW China. Sci. China Ser. D Earth Sci. 49, 154–162.

Lim, B., Cachier, H., 1996. Determination of black carbon by oxidation and thermal treatment in recent marine and lake sediments and Cretaceius–tertiary clays. Chem. Geol. 131, 143–154.

Liu, W.G., Huang, Y.S., An, Z.S., Clemens, S.C., Li, L., Prell, W.L., Ning, Y.F., 2005. Summer monsoon intensity controls C_4/C_3 plant abundance during the last 35 ka in the Chinese Loess Plateau: carbon isotope evidence from bulk organic matter and individual leaf waxes. Palaeogeogr. Palaeoclimatol. Palaeoccol. 220, 243–254.

Liu, L., Song, Y., Cui, L.L., Hao, Z.G., 2013. Stable carbon isotopic composition of black carbon in surface soil as a proxy for reconstructing vegetation on the Chinese Loss Plateau. Palaeogeogr. Palaeoclimatol. Palaeoecol. 388, 109–114.

Lourantou, A., Lavric, J.V., Köhler, P., Barnola, J.-M., Paillard, D., Michel, E., Raynaud, D., Chappellaz, J., 2010. Constraint of the CO_2 rise by new atmospheric carbon isotopic measurements during the last deglaciation. Glob. Biogeochem. Cycles 24, GB2015. http://dx.doi.org/10.1029/2009GB003545.

Lu, Y., Prescott, J.R., Robertson, G.B., Hutton, J.T., 1987. Thermoluminescence dating of the Malan loess at Zhaitang, China. Geology 15, 603–605.

Lu, Y.C., Wang, X.L., Wintle, A.G., 2007. A new OSL chronology for dust accumulation in the last 130,000 yr for the Chinese Loess Plateau. Quat. Res. 67, 152–160.

Masiello, C.A., 2004. New directions in black carbon organic geochemistry. Mar. Chem. 92, 201–213.

Ode, D.J., Tieszen, L.L., Lerman, J.C., 1980. The seasonal contribution of C_3 and C_4 plant species to primary production in a mixed prairie. Ecology 61, 1304–1311.

O'Leary, M.H., 1988. Carbon isotopes in photosynthesis. Bioscience 38, 328–336.

Rao, Z.G., Chen, F.H., Chao, J., Zhang, P.Z., Zhang, P.Y., 2005. Variation of soil organic carbon isotope and C3/C4 vegetation type transition in the western Loess Plateau during the last glacial and Holocene periods. Quat. Sci. 25, 107–114 (In Chinese with English abstract).

Rao, Z.G., Chen, F.H., Cheng, H., Liu, W.G., Wang, G.A., Lai, Z.P., Bloemendal, J., 2013. High-resolution summer precipitation variations in the western Chinese Loess Plateau during the last glacial. Sci Rep 3:2875. http://dx.doi.org/10.1038/srep02785.

Sage, R.F., Wedin, D.A., Li, M., 1999. The biogeography of C4 photosynthesis: patterns and controlling factors. In: Sage, R.F., Monson, R.K. (Eds.), C4 Plant Biology. Academic, San Diego, pp. 313–373.

Shui, T., 2001. Papers on the Bronze Age Archaeology of Northwest. China Science Press, Beijing (in Chinese).

Sun, A.Z., Feng, Z.D., Ma, Y.Z., 2010. Vegetation and environmental changes in western Chinese Loess Plateau since 13.0 ka BP. J. Geogr. Sci. 20, 177–192.

Tang, L.Y., Li, C.H., An, C.B., Wang, W.G., 2007. Vegetation history of the western Loess Plateau of China during the last 40 ka based on pollen record. Acta Palaeontol. Sin. 46 (1), 45–61 (in Chinese with English abstract).

Turney, C.S.M., Bird, M.I., Roberts, R.G., 2001. Elemental $\delta^{13}C$ at Allen's Cave, Nullarbor Plain, Australia: assessing post-depositional disturbance and reconstructing past environments. J. Quat. Sci. 16, 779–784.

Wang, G.A., Han, J.M., Liu, T.S., 2003. The carbon isotopic composition of C3 herbaceous plants in loess area of North China. Sci. Chin. 46, 1069–1076 (Series D).

Wang, X., Peng, P.A., Ding, Z.L., 2005. Black carbon records in Chinese Loess Plateau over the last two glacial cycles and implications for paleofires. Palaeogeogr. Palaeoclimatol. Palaeoecol. 223, 9–19.

Wang, Y.J., Cheng, H., Edwards, R.L., Kong, X.G., Shao, X.H., Chen, S.T., Wu, J.Y., Jiang, X.Y., Wang, X.F., An, Z.S., 2008a. Millennial- and orbital-scale changes in the East Asian monsoon over the past 224,000 years. Nature 451, 1090–1093.

Wang, G.A., Feng, X., Han, J., Zhou, L., Tan, W., Su, F., 2008b. Paleovegetation reconstruction using $\delta^{13}C$ of soil organic matter. Biogeosciences 5, 1325–1337.

Wang, X., Ding, Z.L., Peng, P.A., 2012. Changes in fire regimes on the Chinese Loess Plateau since the Last Glacial Maximum and implications for linkages to paleoclimate and past human activity. Palaeogeogr. Palaeoclimatol. Palaeoecol. 315-316, 61–74.

Wang, X., Cui, L.L., Xiao, J.L., Ding, Z.L., 2013a. Stable carbon isotope of black carbon in lake sediments as an indicator of terrestrial environmental changes: an evaluation on paleorecord from Daihai Lake, Inner Mongolia, China. Chem. Geol. 347, 123–134.

Wang, X., Xiao, J.L., Cui, L.L., Ding, Z.L., 2013b. Holocene changes in fire frequency in the Daihai Lake region (north-central China): indications and implications for an important role of human activity. Quat. Sci. Rev. 59, 18–29.

Wittmer, M.H.O.M., Auerswald, K., Bai, Y.F., Schäufele, R., Schnyder, H., 2010. Changes in the abundance of C3/C4 species of Inner Mongolia grassland: evidence from isotopic composition of soil and vegetation. Glob. Chang. Biol. 16, 605–616.

Xiao, J.L., Wu, J.T., Si, B., Liang, W.D., Nakamura, T., Liu, B.L., Inouchi, Y., 2006. Holocene climate changes in the monsoon/arid transition reflected by carbon concentration in Daihai Lake of Inner Mongolia. The Holocene 16, 551–560.

Yang, S.L., Ding, Z.L., 2008. Advance-retreat history of the East-Asian summer monsoon rainfall belt over northern China during the last two glacial-interglacial cycles. Earth Planet. Sci. Lett. 274, 499–510.

Yang, S.L., Ding, Z.L., Wang, X., Tang, Z.H., Gu, Z.Y., 2012. Negative $\delta^{18}O$-$\delta^{13}C$ relationship of pedogenic carbonate from northern China indicates a strong response of C3/C4 biomass to the seasonality of Asian monsoon precipitation. Palaeogeogr. Palaeoclimatol. Palaeoecol. 317-318, 32–40.

Yang, S.L., Ding, Z.L., Li, Y.Y., Wang, X., Jiang, W.Y., Huang, X.F., 2015. Warming-induced northwestward migration of the East Asian monsoon rain belt from the Last Glacial Maximum to the mid-Holocene. Proc. Natl. Acad. Sci. U. S. A. 112 (43), 13178–13183.

Zech, M., Zech, R., Glaser, B., 2007. A 240,000-year stable carbon and nitrogen isotope record from a loess-like palaeosol sequence in the Tumara Valley, Northeast Siberia. Chem. Geol. 242, 307–318.

Zech, R., Zech, M., Markovic, S., Hambach, U., Huang, Y., 2013. Humid glacials, arid interglacials? Critical thoughts on pedogenesis and paleoclimate based on multi-proxy analyses of the loess-paleosol sequence Crvenka, Northern Serbia. Palaeogeogr. Palaeoclimatol. Palaeoecol. 387, 165–175.

Zhang, J.H., Wang, X.J., Qian, Y.H., Pei, S.Y., 2007. Environmental factor analysis of grassland fire in Qinghai Province. J. Nat. Disaster 16, 71–75 (in Chinese with English abstract).

Zhao, S.J., Ding, Z.L., 2014. Changes in plant diversity on the Chinese Loess Plateau since the Last Glacial Maximum. Chin. Sci. Bull. 59, 4096–4100.

Zheng, S.X., Shangguan, Z.P., 2007. Foliar $\delta^{13}C$ values of nine dominant species in the Loess Plateau of China. Photosynthetica 45, 110–119.

Zhou, B., Shen, C.D., Zheng, H.B., Zhao, M.X., Sun, Y.M., 2009. Vegetation evolution on the central Chinese Loess Plateau since late quaternary evidenced by elemental carbon isotopic composition. Chin. Sci. Bull. 54, 2082–2089.